Pyridylthiazoles: Highly Luminescent Heterocyclic Compounds

Ulrich-W. Grummt,*,† Dieter Weiss,‡ Eckhard Birckner,† and R. Beckert‡

Institut für Physikalische Chemie der Friedrich-Schiller-Universität Jena, Helmholtzweg 4, D 07743 Jena, Germany, Institut für Organische und Makromolekulare Chemie der Friedrich-Schiller-Universität Jena, Humboldtstrasse 10, D 07743 Jena, Germany

Received: November 1, 2006; In Final Form: December 8, 2006

Absorption, fluorescence, and fluorescence excitation spectra of two substituted [(5-methyl-2-pyridine-2′-yl-1,3-thiazole-4-yl)oxy]acetic acid and its methyl ester (2,2′-pyridylthiazoles) are studied at various pH values in aqueous solution. The acid exhibits $pK_a(1) = 2.10 \pm 0.07$ and $pK_a(2) = 3.45 \pm 0.03$, whereas the ester $pK_a = 1.93 \pm 0.03$. The protonation site is the pyridyl-nitrogen. When protonated, the cisoid conformer is the most stable; however, the transoid conformer is more stable in the deprotonated form. Fluorescence quantum yields close to unity are found. Large Stokes shift values are explained by the shortening of the inter-ring bond in the excited state. These compounds may be useful for metal sensing and as laser dyes.

Introduction

Most small heterocyclic compounds are non- or at least very weakly fluorescent. This applies in particular to 2,2′-bipyridine, which is one of the most thoroughly investigated and frequently applied bidentate heterocyclic ligands.[1] We have found that replacing one pyridyl ring of 2,2′-bipyridine by a (substituted) thiazolyl ring leads to a highly fluorescent compound with the same structural motif for complexation.

Pyridyl-substituted thiazoles are not among the most investigated heterocycles. Nevertheless, some interesting applications as pharmaceuticals do exist. Depending on the substitution pattern, they may have fungicidal activity[2] or they may serve as inhibitors of 5-lipogenase.[3] From the viewpoint of coordination chemistry, these compounds are diazadiene ligands and should be capable of forming complexes with metal ions. The highly fluorescent nature of the ligand can be advantageous for the spectroscopic investigation of complex formation and dissociation equilibria. In nature, substituted thiazoles are quite common because they can be synthesized by cyclization from cysteine. The most popular example is oxyluciferin, a benzothiazole-substituted thiazole that acts as the bioluminescence emitter in fireflies.[4] The emission of this compound is quite complex, and different emission colors can be generated.[5] In this work, our interest is twofold. We seek to learn more about the fluorescence of thiazole derivatives as well as to generate a new ligand with the highest luminescence quantum yield possible to obtain a new antenna molecule for photoelectric devices.

In this paper, we focus on the acid−base properties of 5-methyl-2-pyridine-2′-yl-1,3-thiazole-4-yl-oxyacetic acid **(PTOA)** and its methyl ester as well as on the fluorescence properties of these molecules. The chemical structures are depicted in Scheme 1. We will report on quantum chemical calculations carried out in order to interpret the experimental findings, in particular, the unusually large Stokes shift.

Completely analogous results have been obtained with a compound lacking the methyl substituent. This compound, however, has not been obtained in highly pure form. It follows from a comparison of the absorption spectra with the fluorescence excitation spectra and from the mutual independence of the emission and excitation spectra of the excitation and emission wavelengths that this compound is free from intervening absorbers in the relevant region. Therefore, those results are nevertheless reliable, and they fully support the conclusions reported here for **PTOA**.

SCHEME 1: Structure and Numbering Scheme

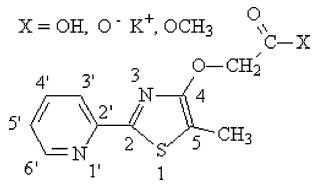

Experimental and Methods

Syntheses. *5-Methyl-2-pyridine-2′-yl-1,3-thiazole-4-ol.* The heterocyclic body was synthesized with a method described in the literature.[6] In an inert atmosphere, pyridine-2-carbonitrile (5.2 g, 0.05 mol) was treated with mercaptolactic acid (5.3 g, 0.05 mol) and 1 mL of pyridine. The mixture was stirred for 4 h at 100 °C. During this time, the nearly colorless mixture became turbid and a yellow mass precipitated. This yellow mass was collected by filtration and washed with methanol. Recrystallization from ethanol formed yellow needles. Yield: 6.7 g (69%), mp = 229 °C (Lit. 230 °C)

Methyl[(5-methyl-2-pyridine-2′-yl-1,3-thiazole-4-yl)oxy]acetate. Hydroxythiazole (5.0 g, 26.0 mmol) and potassium carbonate (3.9 g, 28.2 mmol) were suspended in acetonitrile. To this dark-yellow suspension was added a slight excess of methylbromoacetate (4.1 g, 26.9 mmol) dissolved in acetonitrile. This mixture was stirred overnight, and the solvent was then removed under vacuum. The dry residue was purified by column chromatography on silica gel (toluene/ethyl acetate 5:1). Yield: 5.6 g (81%), mp = 79.7 °C. ^{1}H NMR (250 mHz, $CDCl_3$, δ): 2.39 (s, 3 H), 3.80 (s, 3 H), 4.95 (s, 2 H), 7.35 (m, 1 H), 7.73 (m, 1 H), 8.55 (m, 1 H). ^{13}C NMR (250 mHz, $CDCl_3$, δ): 9.45, 51.99, 66.51, 110.50, 118.67, 123.79, 136.77, 149.29,

* To whom correspondence should be addressed. E-mail: cug@uni-jena.de.
† Institut für Physikalische Chemie.
‡ Institut für Organische und Makromolekulare Chemie.

10.1021/jp0672003 CCC: $37.00
Published on Web 01/25/2007

151.34, 158.62, 159.82, 170.06. IR (KBr): 2956, 1755, 1583, 1547, 1207, 1155, 1147 cm^{-1}. Anal. Calcd for $C_{12}H_{12}N_2O_3S$ (264.3): C, 54.53; H, 4.58; N, 10.60; S, 12.13. Found: C, 54.48; H, 4.69; N, 10.57; S, 11.97.

5-Methyl-2-pyridine-2-yl-1,3-thiazole-4-yl-oxyacetate-potassium salt. The methyl ester (0.8 g, 3.0 mmol) was dissolved in 5 mL of ethanol and stirred. To this solution was added a solution of potassium hydroxide (0.17 g, 3.0 mmol) in 1 mL of water. After a few minutes, a nearly white solid precipitated. The mixture was stirred overnight, and the solid product was filtered off, washed with ethanol, and dried. Yield: 0.55 g (88%) mp = 274.4 (decomp.). ^{1}H NMR (250 mHz, D_2O, δ): 2.15 (s, 3 H), 4.48 (s, 2 H), 7.22 (m, 1 H), 7.65 (m, 2 H), 8.17 (m, 1 H). ^{13}C NMR (250 mHz, D_2O, δ) 8.63, 68.82, 111.69, 119.31, 124.58, 138.19, 148.50, 149.48, 158.42, 158.77, 176.86. IR (KBr): 3342, 1598, 1550, 1314, 1151 cm^{-1}. MS (micro-ESI neg. in methanol): 249 (M−H).

Spectroscopic Techniques. UV−vis spectra were recorded on a Perkin-Elmer Lambda 16 spectrophotometer. Fluorescence measurements were performed on a Perkin-Elmer LS 50 or a Fluorolog III (SPEX) spectrometer. The fluorescence quantum yields were determined relative to quinine sulfate (purum, Fluka) in 0.1 N sulfuric acid (pro analysi, Laborchemie Apolda) as the fluorescence standard ($\varphi_f = 0.55$, $n^D_{20} = 1.333$) according to ref 7.

Fluorescence lifetimes were determined by time-correlated single photon counting using an FL900CD fluorometer (Edinburgh Analytical Instruments). Fluorescence kinetics analyses requiring a higher time resolution were obtained from a homemade single photon counting apparatus based on a Becker & Hickel SPC430, Ti-sapphire second harmonic excitation (90 fs pulsewidth) and a Hamamatsu channel plate gated photomultiplier with a 35 ps rise time. Details of the apparatus and the data evaluation are given in ref 8.

The pH was obtained by means of an HI9318 (Hanna Instruments) with a glass electrode InLab 424 (Mettler Toledo). Potassium dihydrogenphosphate disodium hydrogen phosphate buffer (HI 7007, pH 7.01) and potassium hydrogen phthalate buffer (HI 7004, pH 4.01) were used for calibration. For the spectroscopic pK_a determination, aliquots of a stock solution and aqueous buffer solution were mixed. The ionic strength of the latter had been adjusted to 0.2 M using aqueous KCl so that the ionic strength of the sample in the final solution was 0.1 M (at pH > 1).

For pK_a* determination, the wavenumbers of the electronic 0−0 transitions were determined from the intersection point between the normalized absorption and fluorescence spectra, which were recorded vs wavenumber. All solvents applied in the measurements were of spectroscopic grade. Solutions with the lowest and highest pH were tested for their stability and reversibility of the spectral changes upon pH variation over a period of at least 24 h. No spectral changes were observed, and the pH-induced changes were proven to be completely reversible.

Stopped flow pH jump experiments were performed with the help of an SX18MV spectrometer (Applied Photophysics Ltd.), which exhibited a dead time of roughly 1 ms.

Methods. Most quantum chemical calculations were performed using Gaussian 98 revision A.11.4.[9] Structures were fully optimized at the B3LYP/6-311+G(d) level if not otherwise stated. The same model chemistry was used for the calculation of the torsional profiles, where all coordinates except one fixed dihedral angle were optimized. The stationary points were again fully optimized without constraints. The zero-point energies from the frequency calculations were not scaled. All energies are given in units of kJ mol^{-1}, bond lengths in pm and angles in degrees. RHF/6-311+G(d) and RCIS/6-311+G(d) model chemistries were applied to compare the ground state and excited-state geometries and dipole moments of the model compound 2-pyrid-2′-yl-5-methoxy-1,3-thiazole. Tomasi's polarized dielectric continuum model (SCRF=PCM) implemented in the GAUSSIAN 03 suite (revision D.01) was applied for the calculation of the Gibbs solvation free energies after full geometry optimization in the solvent water.

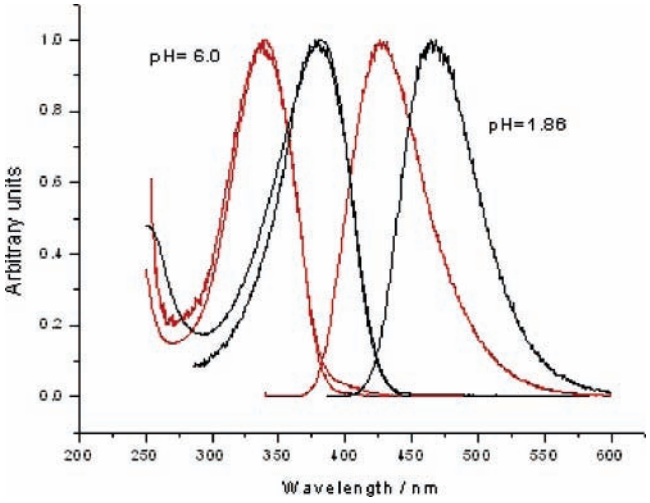

Figure 1. Absorption, fluorescence and fluorescence excitation spectra of **PTOA** anion (red) and cation (black).

TABLE 1: Absorption and Fluorescence Maxima and Stokes Shifts of PTOA in Solvents of Different Polarity

solvent	λ_{max} (abs) [nm]	λ_{max} (fluor) [nm]	Stokes shift [cm^{-1}]
hexane	340	398	4286
toluene	341	409	4876
dioxane	342	408	4730
butyronitrile	340	413	5199
propionitrile	341	417	5345
acetonitrile	340	411	5081
ethanol	346	419.5	5064
water	339	412.5	5256

The difference of dipole moments, $\Delta\mu$, was obtained from the slope of a plot after Lippert[10]

$$\Delta\nu_{00} = \frac{2(\Delta\mu)^2}{\alpha' hc\, 4\pi\epsilon_0}\left[\frac{\epsilon - 1}{2\epsilon - 1} - \frac{n^2 - 1}{2n^2 + 1}\right] \text{ with } \alpha' = \frac{1}{2}a^3 \quad (1)$$

where α' is the polarization volume and a is the radius of the solvent cage.

All fitting procedures were performed with a general nonlinear regression program based on the method described in ref 11.

Results and Discussion

Absorption and Emission Spectra. Figure 1 shows the normalized absorption, fluorescence, and fluorescence excitation spectra of **PTOA** in neutral and acidic aqueous solution. The very small absorption of the neutral form in the long wavelength tail is significant because it is not detected in the excitation spectrum. This absorption is due to the protonated form, which exhibits a lower fluorescence quantum yield, see below.

The Stokes shift of more than 5000 cm^{-1} (cf. Table 1) is comparatively large for a molecule of the given small size. Three potential explanations may be taken into consideration as a

reason for the large Stokes shift: (i) strong charge transfer (CT) nature of the S_1 state, (ii) excited-state proton transfer (ESPT), or (iii) significant geometry changes in the S_1 state.

We can rule out CT due to the almost negligible solvent effect on the absorption wavelength, cf. Table 1. Although still small, the solvent effect on the emission wavelength is slightly more significant. Thus, an estimate of the dipole moment difference can be obtained from the variation of the Stokes shift with respect to solvent polarity according to eq 1. With the solvents given in Table 1 (excluding water) and a cavity radius of 300 pm obtained from the molecular volume ($V_{mol} = 70.9$ cm^3/mol), we obtain a difference of 1.6 D.

The Förster cycle commonly used for the determination of pK_a changes upon excitation is not applicable in the present case because it requires rapid establishment of the acid−base equilibrium in the excited state (the resulting ΔpK_a would be $= 5.5$). The cation protonated at the pyridine nitrogen exists preferentially in the cisoid conformation (vide infra), whereas the free base is transoid. The transoid → cisoid isomerization is generally improbable in the excited state due to the NEER principle[12] and, particularly, due to the Imamura Hoffman[13] rules. Without explicitely calculating the barrier in the excited state, we can safely conclude from the shortening of the linkage between the heterocyclic rings that this barrier is significantly higher than that in the ground state.

Because of the overlap of the fluorescence spectra of the cation and the anion, it is not possible to detect the sole fluorescence of the cationic species. The cationic form can be excited selectively, which affords the possibility of applying the Weller method for the determination of the pK_a difference according to the equation

$$\mathrm{pH} - \mathrm{p}K_s^* = lg\left(\frac{I_f^0\, I_{abs,AH}}{I_f\, I_{abs,AH}^0} - 1\right) \qquad (2)$$

where I_f and I_{abs} are the fluorescence and absorption intensities, respectively. The superscript 0 refers to a pH where the dissociated form is negligible in both states. We obtained ΔpH ≈ 0.02, which implies that there is essentially no shift of the dissociation equilibrium observable. Also, variation of the excitation and emission wavelengths gives no hint that fluorescence of the protonated species is generated upon exciting the unprotonated one. Thus, ESPT can also be excluded as a major relaxation channel of the S_1 state. The fact that the same pK_a values are found in both the pH-dependent absorption and emission spectra confirms again the absence of any excited-state acid−base equilibration.

Any charge-transfer character of an electronic transition should manifest itself by a significantly larger solvent dependence of the Stokes shift than what was observed. The small dipole moment change obtained upon excitation must be regarded as only a crude estimate because eq 1 holds for the anomalous Stokes shift given by the difference of the 0−0-transitions. The dipole moments obtained from ground-state (RHF/6-311+g(d)) and excited-state (RCIS/6-311+g(d)) geometry optimizations of 2-(2′-pyridyl)-4-methoxy-1,3-thiazole **PMTh** were 0.40 (1.28) and 0.30 (1.13) D, respectively. The values in parentheses refer to the unsubstituted **PTh,** cf. Supporting Information. Thus the donor substituent reduces the dipole moment in the ground state. Whereas the magnitude remains nearly unchanged upon excitation, the direction is reversed. This means that charge transfer contributes to the Stokes shift, although only to a minor extent. The anomalous Stokes shift, not visible in the vibrationally unresolved spectra, is expected to be comparatively small. Excitation and emission spectra of the ester in solid solution at 77 K where solvent relaxation is frozen reveal $\Delta\nu = 3950$ cm^{-1} (4990 cm^{-1}) in *n*-butyronitrile and $\Delta\nu = 3650$ cm^{-1} (4180 cm^{-1}) in methylcyclohexane. Stokes shifts from fluid solution at room temperature are given in parentheses for comparison. Consequently, we must conclude that a significant geometric change is the reason for the large Stokes shift and solvent relaxation plays a minor role. This conclusion will be confirmed by quantum chemical calculations as outlined below.

TABLE 2: Photophysical Data, k_f, Experimental Radiative Decay Constant $k_f = \phi_f/\tau_f$, k_f(SB), Radiative Rate Constant According to Strickler and Berg

	pH	τ_f [ns]	ϕ_f	k_f [ns^{-1}]	k_f(SB) [ns^{-1}]
ester	>6	5.88	0.95	0.16	0.15
	≈1	2.70	0.39	0.14	0.11
acid	>6	5.40	0.91	0.17	0.14
	≈1	4.07	0.63	0.15	0.13

Fluorescence Kinetics. Natural fluorescence lifetimes and quantum yields together with radiative rates determined either from experimental data or the Strickler and Berg equation are given in Table 2.

The coinciding of k_f and k_f(SB) values provide evidence for the identity of the state populated by absorption as well as the emitting one. Both the protonated and unprotonated forms of the methyl ester show a clean, singly exponential fluorescence decay with $\tau_f = 4.07$ ns (at pH 1.1) and $\tau_f = 5.40$ ns (at pH 6.39), respectively. There is no variation with either excitation or emission wavelength. A smooth first-order decay and wavelength independence is also observed, with the protonated acid and the anion at pH $\approx$ 1 and pH > 6, respectively. We obtained $\tau_f = 2.70$ ns (at pH 1.1) and $\tau_f = 5.88$ ns (at pH 6.42). At the isoelectric point (pH 2.7), three species are expected to contribute to fluorescence. The kinetic analysis of the emission under a variation of the emission and excitation wavelength indeed yield (at least) three species. However, the lifetimes measured with the cation and the anion were not recovered at pH 2.7. Excitation at 400 nm, where the N-protonated forms can be selectively excited, reveals two components with $\tau_f = 2.00$ and 4.9 ns. A third lifetime ($\tau_f = 4.2$ ns) becomes observable with lower wavelength excitation. At any rate, the kinetic analyses support the assumption that more than one long wavelength emitting and absorbing species is present without specifying their identities. It is possible that the thermodynamically less stable conformers cannot be neglected near the isoelectric point. This would increase the number of expected absorbing and emitting species and render the system exceedingly complex. More detailed investigations are the subject of future work.

Static fluorescence quenching was observed with a series of heavy metal ions. As an example, we present a Stern−Volmer plot showing the nonlinear dependence that can be fitted well to a second-order polynomial (Figure 2). This behavior is consistent with a 1:2 coordination. Further studies with the aim of determining the complex formation constants are in progress.

pH Equilibria in the Ground State. Figure 3 shows a set of absorption spectra measured in aqueous solutions at various pH values. The absence of isosbestic points gives evidence that at least three species contribute to the absorption spectrum. Principal component analysis reveals that 99.997% of the total variance can be described by three components. Figure 4 shows the abstract eigenspectra derived from the set shown in Figure 3. Because the carboxylate group is electronically decoupled from the π-system, only minor absorption changes are expected

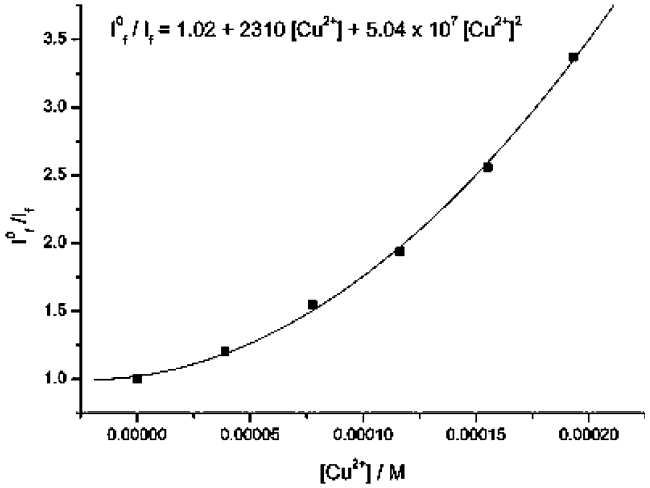

Figure 2. Stern−Volmer plot of the fluorescence quenching **of PTOA** by Cu^{2+} ions.

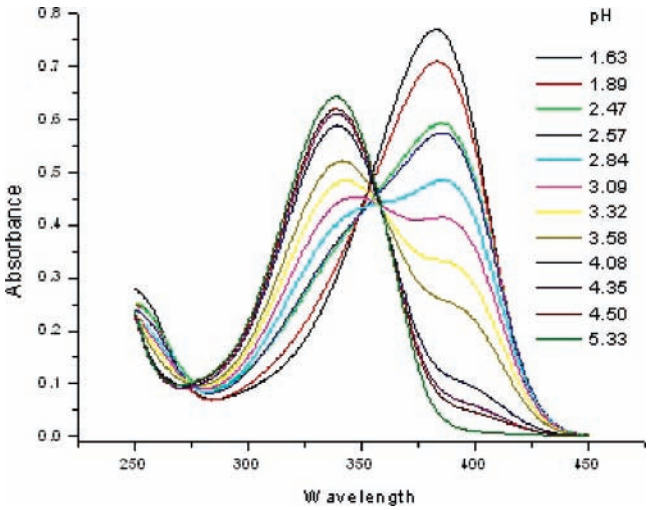

Figure 3. Set of absorption spectra for **PTOA** obtained at various of pH values.

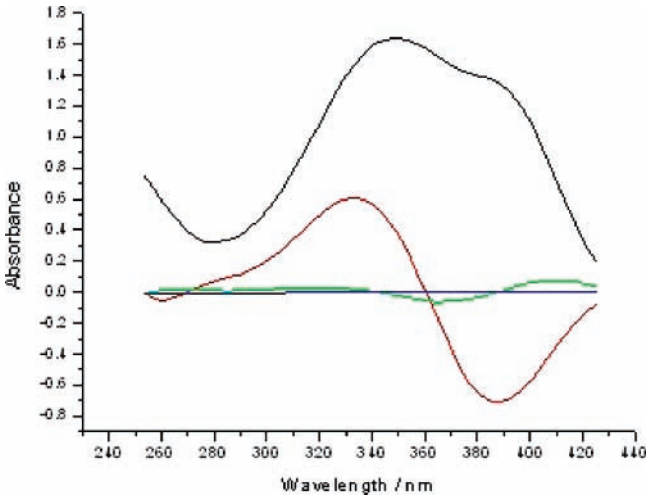

Figure 4. Abstract eigenspectra obtained from the set shown in Figure 3.

upon protonation of this group. Nevertheless, the small but significant third eigenspectrum suggests that both protonation equilibria should be resolvable from the data set.

Because we do not observe any additional spectral changes upon further increasing the pH, the absorption peak at 338 nm (pH > 3) must be assigned to the anion. The maximum at 383 nm (pH < 3), on the other hand, must be assigned to a protonated compound. It is less straightforward to unequivocally identify the third species. The neutral molecule might exist in the uncharged form, as given in the formula (Scheme 1), or as a zwitterion. Furthermore, rotational isomerism around the bond linking the heterocyclic rings must be taken into consideration as discussed below. (Conformational equilibria of the side chain are not considered because they are not expected to influence the spectral behavior. Theory predicts the existence of further metastable species in the gas phase with hydrogen bridges from the carboxylic acid to either of the N atoms.)

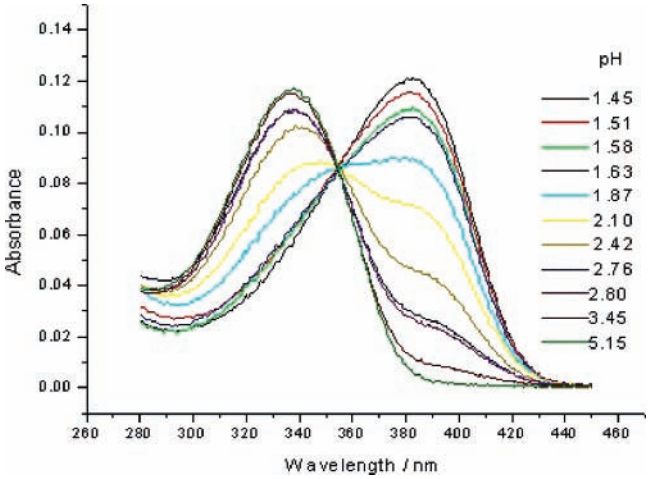

Figure 5. pH-dependent absorption spectra of the ester.

All sets of spectra can be fitted to a model composed of two consecutive acid−base dissociation equilibria

$$AH_2^+ \leftrightarrows AH + H^+ \leftrightarrows A^- + 2H^+$$

$$I(\lambda) = \frac{I_{AH_2^+}(\lambda) + I_{AH}(\lambda) \times 10^{pH-pK_1} + I_{A^-}(\lambda) \times 10^{2pH-pK_1-pK_2}}{1 + 10^{pH-pK_1} + 10^{2pH-pK_1-pK_2}} \quad (3)$$

where I represents the absorptivity in the case of the absorption spectra and for the relative fluorescence intensity (counts) in the case of the fluorescence and fluorescence excitation spectra. The spectra recorded at the extremal pH values were first chosen as fixed parameters (extinction coefficients or relative fluorescence intensities) for the cationic and the anionic species. From a global fit of the entire sets of spectra to eq 3, guesses of the spectra of the intermediate species were obtained in addition to the parameters pK_1 and pK_2. Final optimization of all spectral parameters leaves the results unchanged within the limit of error. To unequivocally assign the two consecutive equilibria to specific molecular sites, we have also investigated the acid−base equilibrium of the ester (in acetonitrile/water 1:1). Figure 5 shows a set absorption spectra recorded at varied of pH values. Principal component analysis reveals that 99.98% of the total variance is reproduced by two components. Figure 6 shows the abstract eigenspectra.

From a global fit, a pK_a value of 1.93 ± 0.01 was obtained that agrees with single wavelength fits. For instance, at the maxima of either species at 338 and 380 nm, the pK_a values were 1.91 ± 0.02 and 1.99 ± 0.06, respectively (Table 3).

Consequently, the lower pK_a obtained for the acid must be assigned to the pyridinium moiety. The second pK_a refers to the acetic acid substituent. Titration of the salt (6.5 mM in water) with 0.1 M perchloric acid gave a pK_1 of 3.46. (The second

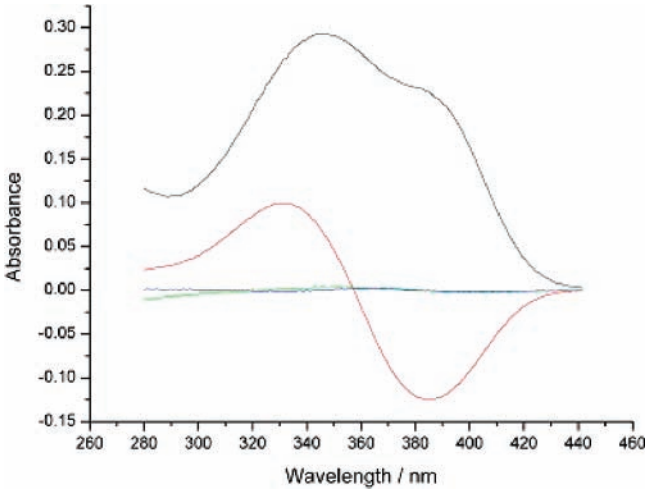

Figure 6. Abstract eigenspectra obtained from the set shown in Figure 5.

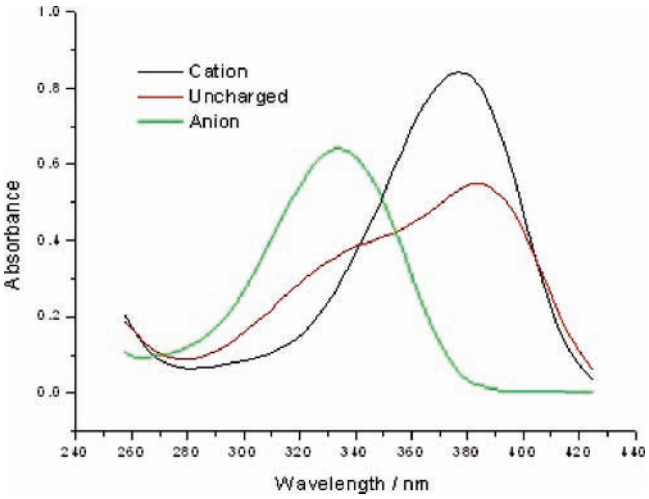

Figure 7. Absorption spectra of the cationic, uncharged, and anionic forms of PTOA obtained from a global fit according to eq 3.

TABLE 3: pK_a Values Obtained from pH-Dependent Absorption, Fluorescence, and Excitation Spectra

absorption	3.433 ± 0.003	2.10 ± 0.01
fluorescence	3.47 ± 0.01	1.81 ± 0.11
excitation	3.58 ± 0.07	2.29 ± 0.08

inflection point could not be precisely located because the substance crystallized on the electrode below pH = 4. The pH steps became blurred at a dilution necessary to avoid precipitation.) The value pK_1 = 3.46 coincides remarkably well with the value published for methoxy acetic acid: pK_a = 3.5.[14] However, there is one discrepancy: the absorption spectra of the uncharged species obtained from the fitting procedure (Figure 7) shows its maximum near the maximum of the protonated species. This would suggest that the neutral species exists as a zwitterion with a protonated pyridyl ring, a result that is at variance with the pK_a gradations. A tentative explanation of the discrepancy that could not be confirmed might be the formation of a valence tautomeric lactone with a C^5−O bond (Cf. Supporting Information). Attempts to extract the neutral species with $CHCl_3$ from aqueous solution at pH = 2.7 (mean between pK_{a1} and pK_{a2}) resulted in solutions absorbing at 340 nm.

In dimethyl sulfoxide solvent, the acidic proton is unequivocally attached to the carboxyl group as proven by ^{1}H NMR spectroscopy, in particular, by the observed spin polarization

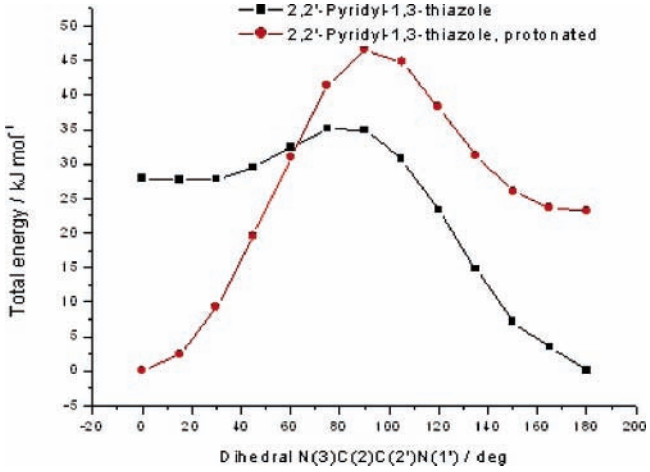

Figure 8. Rotational profiles of **PMTh** and **PH$^+$MTh.**

TABLE 4: Theoretical Gibbs Free Energy of Formation Differences Relative to the Global Minima for the Stationary Points of Pyridyl-methoxythiazole as a Neutral Molecule and as Either Protonated Species

	PMTh		**PyH$^+$MTh**		**PyMThH$^+$**	
	Δ*G* [kJ/mol]	dihedral [deg]	Δ*G* [kJ/mol]	dihedral [deg]	Δ*G* [kJ/mol]	dihedral [deg]
cisoid	25.8	23.5	0	0.0	5.4	0.0
transoid	0	180.0	19.4	180.0	148.4	18.0
transition	37.6	82.8	53.6	92.8	n.d.	
state	30.7	0.0				

transfer between this acidic proton (12.8 ppm) and the neighboring methylene protons (4.9 ppm).

Because the overall protonation/deprotonation step includes an isomerization around the bond linking both heterocycles, there should be a chance to observe this step with the help of the stopped flow technique. However, by far the most spectral changes occur during the primary acid−base reaction, whereas a very small spectral shift corresponds to the subsequent isomerization. This explains why we were unable to record spectral changes after a dead time of about 1 ms with either upward or downward pH jumps.

Quantum Chemical Calculations. Quantum chemical structure elucidations were performed for the unsubstituted pyridylthiazole (**PTh**), the methoxy-substituted pyridylthiazole (**PMTh**), **PTOA**, its protonated and deprotonated forms, and the (hypothetical) lactone. Data for **PTh** and the lactone are given in the Supporting Information. The neutral species as well as the anion of **PTOA** are most stable as transoid conformers in the gas phase, whereas the cation (pyridinium) exist in the cisoid form analogously to 2,2′−bipyridine.[15] The Gibbs free energy difference between both conformers of **PMTh** was calculated to be 25.8 kJ/mol, which corresponds to approximately 10 kT at room temperature. Figure 8 shows the calculated rotational profiles of the neutral and protonated **PMTh** around the dihedral angle N(3)C(2)C(2′)N(1′). Table 4 presents the Gibbs free energies relative to the most stable conformer.

Thus, provided that there are no dramatic differences between the solvation energies of the conformers, the corresponding unstable conformers should not contribute to the absorption spectra to a measurable extent. Because the barrier from cisoid to transoid **PMTh** is only 11.8 kJ/mol, equilibration from the cisoid to transoid conformer is expected to be rapid. The barrier calculated for the formation of the more stable cisoid **PH$^+$MTh** from its transoid precursor is larger (34.2 kJ mol^{-1}). From a

SCHEME 2: Thermodynamic Cycle for the Calculation of pK_a

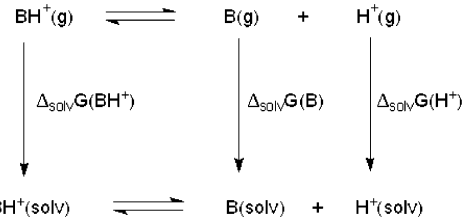

comparison with the acid dissociation constants of its structural constituents, one might expect **PTOA** to exist as a zwitterion in its uncharged form in aqueous solution (pyridinium: pK_a = 5.2;[16] methoxy acetic acid: pK_a = 3.5;[14] 1,3-thiazolinium: pK_a = 2.4[17]). However, analogous to 2,2′-bipyridine, which is a weaker base than pyridine (pK_a = 4.35[16,18]), the basicity of the N-atom in the pyridyl moiety should also be decreased.

Calculations of thermodynamic properties are in favor of the O-protonated species as the uncharged form; however, they do not rule out the existence of the zwitterion as a minor equilibrium constituent in water. The calculated Gibbs solvation free energy for **PTOA** in water was 63.7 kJ/mol, while that of the zwitterion was 228.3 kJ/mol. The difference of 164.6 kJ/mol does not compensate for the difference of the total Gibbs free energies of formation, including thermal and zero-point corrections, which amount to 227.1 kJ/mol.

Theoretical calculations of pK_a are not a trivial task. Various thermodynamic cycles may be used for that purpose.[19] We do not expect to achieve experimental accuracy with our pK_a calculations. Rather, we are interested in discerning between the two possible protonation sites of **PTOA** on a more rigorous basis than on the total SCF energies alone. Hence, we used the simple thermodynamic cycle given in Scheme 2.

The molecular structures of **PMTh**, **PH$^+$MTh**, and **PMThH$^+$** were first optimized in the gas phase. The thermal correction to the Gibbs free energy and the zero-point energy corrections were obtained from frequency calculations with these structures. The total electronic energies were taken from single-point calculations at the B3LYP/6-311++G** level. The optimized gas-phase structures were then used as starting geometries for geometry optimizations in water as the solvent on the B3LYP/6-311+G(d) level using Tomasi's polarized continuum model to obtain the solvation free energies.

It follows from the thermodynamic cycle that the free energy of the acid dissociation in solution is given by

$$\Delta_{soln}G = G(B)_g - G(BH^+)_g + G(H^+)_g + \Delta_{Solv}G(B) + \Delta_{Solv}(H^+) - \Delta_{Solv}G(BH^+) \quad (4)$$

The constant free energy contribution

$$G_{H^+} = G(H^+)_g + \Delta_{Solv}G(H^+) \quad (5)$$

was taken to be 1125.5 kJ/mol (269.0 kcal/mol).[20] In that way, we obtained pK_a values of −1.9 and −5.2 for acid dissociation of the transoid **PH$^+$MTh** and **PMThH$^+$**, respectively. This confirms again that the pyridine moiety is the stronger basic site of the molecule. The solvation free energies calculated for transoid and cisoid **PH$^+$MTh** are −224.2 and −204.21 kJ/mol, respectively. This compensates for the difference in the total SCF energy, including the zero-point energy and thermal correction. The corrected SCF energy is clearly in favor of the cisoid conformer as the most stable one. If one puts confidence in the calculated solvation energies, then it cannot be decided with certainty on the given level of theory which conformer is the more stable one. In spite of this uncertainty, we assume that it is the cisoid conformer because the solvation energy calculations seem more prone to systematic errors. Details are presented in the Supporting Information. The smooth singly exponential fluorescence decay of the cation makes the coexistence of the two species highly improbable.

SCHEME 3: Bond Lengths for the Ground State (Ordinary Type) and the First Excited State (Italics) Molecules

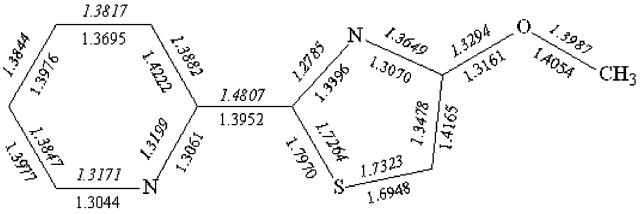

Calculation of the electronic transitions (TD B3LYP/6-31g-(d)) reveals that the π-donor substituent is essential for the high fluorescence quantum yield because it pushes the $\pi-\pi^*$ transition below the $n-\pi^*$ transition. The lowest energy transitions of the unsubstituted **PTh** are predicted to be λ_{max} = 291 nm, f = 0.001, and λ_{max} = 296 nm, f = 0.002 for the transoid and the cisoid conformers, respectively. The corresponding results for **PTOA** are λ_{max} = 320 nm, f = 0.264, and λ_{max} = 311 nm, f = 0.267, in reasonable agreement with the experimental findings. The cationic species are predicted to absorb at λ_{max} = 435 nm, f = 0.171 (transoid), and λ_{max} = 415 nm, f = 0.236 (cisoid).

Time-dependent density functional theory (TDDFT), at least with the simple B3LYP hybrid functional, is inapplicable for the charged species under study. This functional predicts CT transitions with vanishingly small dipole transition moments in the near-infrared region at 1052 and 3528 nm for the anion and zwitterion, respectively. The charge transfer occurs from the carboxylate to the heteroaromatic π-system. It is well-known that TDDFT methods systematically underestimate $\pi-\pi^*$ states with ionic character.[21] TDDFT with the aug-cc-pVTZ basis set systematically overestimates the transition energies; however, we simply rely on their relative magnitudes. These calculations predict the zwitterion to exhibit the longest wavelength transition (λ_{max} = 371 nm, f = 0.437). The undissociated PTOA should exhibit the shortest wavelength absorption, λ_{max} = 271 nm, f = 0.399. The anion is predicted to absorb close to the neutral species, λ_{max} = 291 nm, f = 0.264, and the cation at λ_{max} = 315 nm, f = 0.461.

Scheme 3 shows a comparison of the bond lengths in the ground state and the S_1 state of **PMTh** as a model compound. By far the most significant change is the shortening of the carbon−carbon bond linking the two heterocycles. All four adjacent bonds are lengthened upon excitation. Bond angles are predicted to remain unchanged to within 1°.

The Stokes shift resulting from this geometry change is calculated as $\Delta\nu_{00}$ = 3890 cm^{-1} (TD RB3LYP/6-31G(d)), which is in reasonable agreement with the experimental value.

Conclusion

PTOA is a highly fluorescent bidentate ligand. According to calculations, the alkoxy substituent is essential for the longest wavelength transition. This group causes a considerable bathochromic shift with respect to the unsubstituted **PTh** due to its π-donation ability.

The most stable conformer of the anionic or undissociated neutral forms is the transoid one. Protonation occurs at the pyridyl-nitrogen. The protonated molecule is assumed to be most stable in the cisoid conformation, although the energy difference between both conformers might level off in water, as suggested by the calculated solvation free energies.

Global analyses of the pH-dependent absorption, emission, and excitation spectra reveal $pK_a(1) = 2.10 \pm 0.07$ and $pK_a(2) = 3.45 \pm 0.03$ as weighted mean values with an isoelectric point at pH = 2.8. Acid−base equilibria are not established in the excited state due to a large rotational barrier.

According to the pK_a difference and based on ^{1}H NMR experiments, the zwitterionic species has been ruled out as a major equilibrium constituent.

Large Stokes shifts, mainly due to geometric rearrangments, are observed for the anion, the uncharged molecule, and the methyl ester as well as for the protonated molecule. The vanishingly small overlap of the absorption with the fluorescence spectra, the high fluorescence quantum yield, and the comparatively large lifetime connected with good photochemical stability should qualify these compounds as valuable laser dyes.

Complexation with heavy metal ions leads to efficient static fluorescence quenching, which may be exploited for sensing purposes. The oxyacetic acid side chain offers the possibility of immobilization.

Supporting Information Available: Unsubstituted **PTh**, formation of a valence tautomeric lactone with a C^5−O bond, data for **PTh** and the lactone, and solvation energy calculations (WPD). This material is available free of charge via the Internet at http://pubs.acs.org.

References and Notes

(1) (a) Kaes, C.; Katz, A; Hosseini, M. W. *Chem. Rev.* **2000**, *100*, 3533. (b) Kalyanasundaram, K. *Photochemistry of Polypyridine and Porphyrin Complexes*; Academic Press: London, 1992

(2) Gusmeroli, M.; Ciapessoni, A.; Bettarini, F.; Osti, S.; Mirenna, L.; Camaggi, G.; Gironda, R. PCT Patent WO 2003050096, 2003.

(3) Kerdesky, F. A.; Holms, J. H.; Moore, J. L.; Bell, R. L.; Dyer, R. D.; Carter, G. W.; Brooks, D. W. *J. Med. Chem.* **1991**, *34*, 2158.

(4) (a) Morton, R. A.; Hopkins, T. A.; Seliger, H. H. *Biochemistry* **1969**, *8*, 1598. (b) White, E. H.; Rapaport, T. A.; Hopkins, T. A.; Seliger, H. E. *J. Amer. Chem. Soc.* **1969**, *91*, 2178.

(5) Dahlke, E. E.; Cramer, C. *J. Phys. Org. Chem.* **2003**, *16*, 336.

(6) Brooks, D. W.; Kerdesky, F. A.; Francis, A. J.; Holms, J. H. PCT Patent WO 90-US676, 1990.

(7) Demas, J. N.; Crosby, G. A. *J. Phys. Chem.* **1971**, *75*, 9912.

(8) Grummt, U.-W.; Pautzsch, T.; Birckner, E.; Sauerbrey, H.; Utterodt, A.; Neugebauer, U.; Klemm, E. *J. Phys. Org. Chem.* **2004**, *17*, 199.

(9) Frisch, M. J.; Trucks, G. W.; Schlegel, H. B.; Scuseria, G. E.; Robb, M. A.; Cheeseman, J. R.; Zakrzewski, V. G.; Montgomery, J. A., Jr.; Stratmann, R. E.; Burant, J. C.; Dapprich, S.; Millam, J. M.; Daniels, A. D.; Kudin, K. N.; Strain, M. C.; Farkas, O.; Tomasi, J.; Barone, V.; Cossi, M.; Cammi, R.; Mennucci, B.; Pomelli, C.; Adamo, C.; Clifford, S.; Ochterski, J.; Petersson, G. A.; Ayala, P. Y.; Cui, Q.; Morokuma, K.; Malick, D. K.; Rabuck, A. D.; Raghavachari, K.; Foresman, J. B.; Cioslowski, J.; Ortiz, J. V.; Stefanov, B. B.; Liu, G.; Liashenko, A.; Piskorz, P.; Komaromi, I.; Gomperts, R.; Martin, R. L.; Fox, D. J.; Keith, T.; Al-Laham, M. A.; Peng, C. Y.; Nanayakkara, A.; Gonzalez, C.; Challacombe, M.; Gill, P. M. W.; Johnson, B. G.; Chen, W.; Wong, M. W.; Andres, J. L.; Head-Gordon, M.; Replogle, E. S.; Pople, J. A. *Gaussian 98*, revisions A.7, B.04; Gaussian, Inc.: Pittsburgh, PA, 1998.

(10) Lippert, E. *Z. Elektrochem.* **1957**, *61*, 962.

(11) Schütz, H.; Stutter, E.; Weller, K.; Petri, I. *Stud. Biophys.* **1984**, *104*, 23.

(12) Laarhoven, W. H. In *Organic Photochemistry*; Padwa A. Ed.; Marcel Dekker: New York, 1987; Vol. 9, p 129.

(13) Imamura, A.; Hoffmann, R. *J. Am. Chem. Soc.* **1968**, *90*, 5379.

(14) Antelo, J. M. A.; Arce, F.; Calvo, P.; Crugeiras, J.; Rios, A. *J. Chem. Soc., Perkin Trans. 2* **2000**, 2109; Reinhardt, L. A.; Sackstedter, K. A.; Cleleland, W. W. *J. Am. Chem. Soc.* **1998**, *120*, 13366; Headley, A. D.; Starnes, S. D.; Wilson, L. Y.; Famini, G. R. *J. Org. Chem.* **1994**, *59*, 8040.

(15) Göller, A.; Grummt, U.-W. *Chem. Phys. Lett.* **2000**, *321*, 399.

(16) Perrin, D. D. *Dissociation Constants of Organic Bases in Aqueous Solutions*; Butterworths: London, 1965.

(17) Eicher, T. *The Chemistry of Heterocycles*; Wiley & Sons: New York, 1995.

(18) Goethals, M.; Platteborze K.; Zeegers-Huyskens T. *Spectrochim. Acta* **1992**, *48A*, 671.

(19) Pliego, J. R., Jr. *Chem. Phys. Lett.* **2003**, *367*, 145.

(20) (a) Liptak, M. D.; Gross, K. C.; Seybold, P. G.; Feldgus, S.; Shields, G. C. *J. Am. Chem. Soc.* **2002**, *124*, 6421. (b) Jang, Y. H.; Goddard, W. A., III; Noyes, K. T.; Sowers, L. C.; Hwang, S.; Chung, D. S. *J. Phys. Chem. B* **2003**, *107*, 344.

(21) (a) Tozer, D. J.; Amos, R. D.; Handy, N. C.; Roos, B. O.; Serrano-Andres, L. *Mol. Phys.* **1999**, *97*, 859. (b) Wanko, M.; Garavelli, M.; Bernardi, F.; Niehaus, T. A.; Frauenheim, T.; Elstner, M. *J. Chem. Phys.* **2004**, *120*, 1674. (c) M. Parac, M.; Grimme, M. *Chem. Phys.* **2003**, *292*, 11.